

EHL-Squeeze in High Loaded Contacts: The Case of Chain CVT Transmissions

Michele Scaraggi* - Leonardo De Novellis - Giuseppe Carbone*
DIMEG-Politecnico di Bari, Italy

We analyze the lubrication conditions at the pin-pulley interface in a Gear Chain Industrial chain CVT. In particular, we focus on the squeeze of oil which occurs as soon as the pin enters the pulley groove. The duration time to complete the squeeze process compared with the running time the pin takes to cover the entire arc of contact is fundamental to determine what actually is the lubrication regime at the interface. Taking into account that for normal CVT operations the time the pin spends in contact with the pulley groove is of about 0.01 s (traveling time), we show that rms surface roughness less than 0.1 μm and squeezing load of about 1kN acting on the pin, corresponding to values adopted in such systems, guarantee a fully lubricated EHL regime at the interface. We also show that during low-velocity CVT operations, the lubrication regime at the interface is determined by a succession of hydrodynamic and mixed lubrication stages in an order strictly related to the squeezing load history.

©2010 Journal of Mechanical Engineering. All rights reserved.

Keywords: continuously variable transmission, elasto-hydrodynamic lubrication, squeeze motion, multibody

0 INTRODUCTION

For the past decades continuously variable transmissions (CVTs) have attracted a steadily increasing interest of the scientific and industrial community as a consequence of their potential to reduce vehicle fuel consumption, greenhouse gases, and polluting emissions. CVTs may also increase the vehicle ride comfort and, in the case of best controlled solutions, also its drivability. Moreover, this kind of mechanical transmissions may enable the engine to follow the so-called economy line: For any given power request the CVT speed ratio can be adjusted to get the highest possible thermal efficiency of the engine [1] to [3]. This is particularly interesting under the perspective of the environmental question. However, the mechanical efficiency of CVTs is still smaller compared with that of the stepped transmissions. Thus, a great deal of research is being carried out in order to improve CVT efficiency and/or utilize CVTs at the best of their performances [4] to [6]. One way to improve the mechanical efficiency is that of optimizing the local traction performances at the chain pin-pulley contact. This approach requires a deep understanding of the lubrication conditions [7] and [8] at the interface, as a first step toward an optimization of the micro- and macrogeometry of surfaces, with the final aim to increase the amount of torque per unit normal force that can

be locally transferred through the pin-pulley interface with the minimum wear. In this paper we focus on the Gear Chain Industrial (GCI) CVT (see Fig. 1 for a schematic of the GCI chain). A squeezing motion of the oil interposed between the pin and pulley surfaces occurs as soon as the pin enters the pulley groove, and it is characterized by a sudden step variation of the normal force acting on the pin, from zero (on the free strand of the chain) to a finite value of order 1 kN.

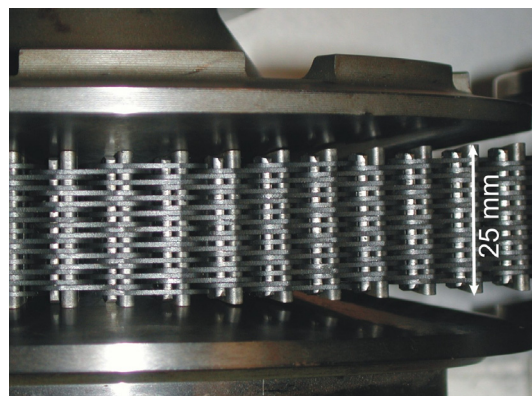


Fig. 1. *The Gear Chain Industrial b.v. (GCI) chain with the pins entering the pulley groove*

This step change of the pin-pulley normal force has been demonstrated by independent

*Corr. Authors' address: DIMEG-Politecnico di Bari, V.le Japigia 182, I-70126 Bari, Italy, m.scaraggi@poliba.it, 245
carbone@poliba.it

investigations both theoretically [5] and [9] to [10] and experimentally [11].

In this work we focus on the theoretical analysis of the oil squeeze at pin-pulley interface during normal and low-speed CVT operations. In particular, the paper is outlined as follows: In Sec. 1 we consider the case of normal CVT operations, where the pin-pulley traveling time (*PPTT*) is typically of about 10^{-2} s. In Sec. 2 we report the calculation results of the pin-pulley interaction performed with an extension to the squeeze contacts of a recently developed mixed lubrication (ML) theory [12] to [13], and show how the interaction evolves for longer *PPTT* under constant normal loads.

Finally, in Sec. 3 we analyze the case of low-speed CVT operations, where the *PPTT* may be of the order 10^{-1} s.

1 THE HIGH-VISCOSITY CENTRAL OIL DIMPLE

The interaction between pin and pulley is characterized by a fast, highly-loaded squeeze of the lubricant film. Contact loads of about 1 kN and pin cross-section area of order 1 mm^2 (average pressure \sim GPa) suggest the EHL regime as the most appropriate to describe the junction behavior, at least until the minimum oil film thickness is large enough to neglect asperity-asperity and asperity-fluid interactions. In [7] to [8] some of us developed the theory and an ad-hoc numerical method for analyzing the pin-pulley squeezing process. Here we show the results for a piezo-viscous and piezo-dense Newtonian lubricant, which qualitatively captures most of the physics for the highly-loaded squeeze of unblended mineral oils [7] and [8]. In Fig. 2 we show the fluid pressure field as function of the contact radius at different time instants.

In the initial stage, see curve at $0.3 \mu\text{s}$ in Fig. 2, the pin/pulley surface deformations are negligible if compared to the lubricant film thickness (the contact shape is still monotonic), therefore the lubrication regime is of the hydrodynamic type with the maximum fluid pressure located at the contact center. This lubrication regime is quickly left as soon as the oil pressure increases. This determines an increase of oil viscosity and the consequent occurrence of an annular pressure spike (see curve at $10 \mu\text{s}$ in Fig. 2) which moves toward the

contact axis with decreasing velocity. This phenomenon, due to the balance between piezo-viscosity, piezodensity and body deformation, is accomplished by the formation of a high-viscosity central dimple, see Fig. 3 for different time instants, which acts as a rigid flat meniscus separating the pin from the pulley and avoids direct asperity-asperity contact.

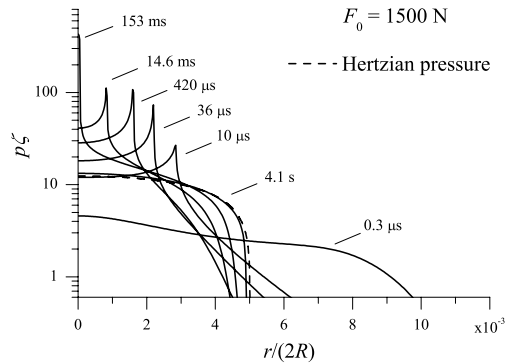


Fig. 2. The dimensionless pressure distribution as function of the dimensionless radial coordinate, in a linear-log diagram. Here R is an equivalent radius of curvature of the bodies, r is the distance from the centre of the contact and ζ is a piezo-viscosity coefficient. Calculations have been performed under an applied constant load $F_0 = 1500 \text{ N}$

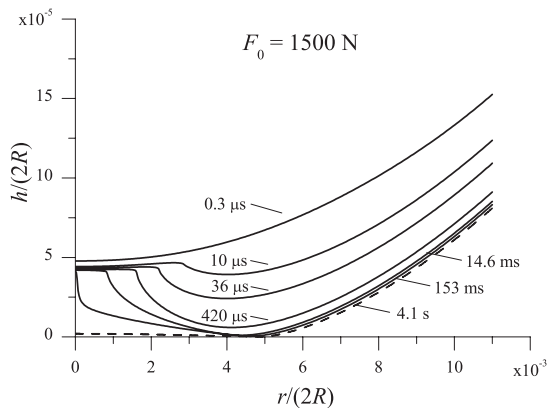


Fig. 3. The dimensionless lubricant film thickness as a function of the dimensionless radial coordinate. R is an equivalent radius of curvature of the bodies, r is the distance from the centre of the contact and ζ is a piezo-viscosity coefficient. Calculations have been performed under an applied constant load $F_0 = 1500 \text{ N}$

Note that the radial position of the annular pressure spike coincides with the radial size of the flat central dimple. Thus the latter disappears when the pressure peak moves in the middle of the junction, see curve at 153 ms in Fig. 2 and in Fig. 3. After the disappearing of the central peak, the EHL model predicts that the fluid pressure slowly converges to a stationary, Hertzian-like solution. Note that EHL theory was found reliable in predicting film thickness also in nanometer-sized oil gap [14], clearly depending on the lubricant properties and surfaces topography. In our case, we limit the validity of the model for film thickness larger than $0.1 \mu\text{m} \approx h_{rms}$ surface roughness, which is also a high enough value to neglect all phenomena connected with nanometer lubrication, see [15] and [16].

However, we have found that the minimum film thickness never reaches the h_{rms} threshold during a squeeze time equal to the $PPTT$, hence the analysis confirms that EHL is the actual pin-pulley lubrication regime (note: In pure squeezing motion as in pure rolling motion, the asperities can be considerably flattened by the fluid action, therefore the value of the effective rms surface roughness can be much lower than the rms value measured in the undeformed configuration. This implies that direct solid-solid interactions may be avoided also during mixed lubrication [17]). In Fig. 4 we show the central and minimum oil film thicknesses as function of time for three different values of normal load, 0.5, 1 and 1.5 kN.

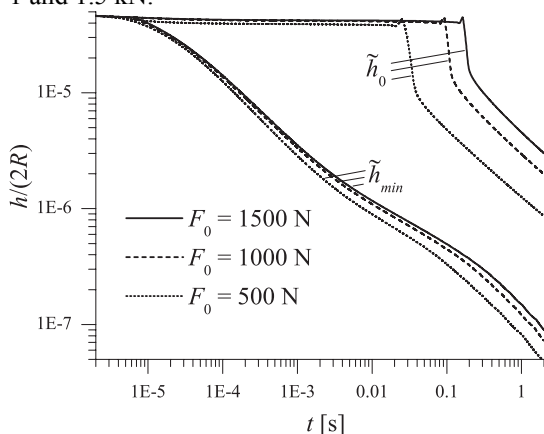


Fig. 4. The dimensionless lubricant minimum $h_{min}/(2R)$ and central film thickness $h_0/(2R)$ as a function of the time in a log-log scale. Calculations have been performed for three applied normal loads $F_0=0.5, 1$ and 1.5 kN

Note how quickly the central gap curves diverge from the minimum gap curves as a consequence of the transition from the hydrodynamic to the elasto-hydrodynamic regime. We also show that the squeeze process speed is higher when the normal load is smaller. This is a consequence of the exponential increase of viscosity due to the lubricant piezo-viscous effect, which, despite the average pressure increases in the contact domain, globally slows down the squeeze motion.

2 THE INFLUENCE OF ROUGHNESS IN HIGH-PRESSURE SQUEEZE MOTION

The influence of roughness in steady-lubrication analysis has been deeply investigated in the last 30 years because of the recognized key importance in a wide range of applications where sub-micrometer oil film thickness is formed [14] and [16]. Nevertheless, tools for the quantitative predictions of mixed lubricated interactions are still lacking, as the main problem in modeling real contacts is that most surfaces of practical interest have surface roughness over a large range of length scales, typically from mm to nm, which results in too many degrees of freedom to be handled by numerical methods [12]. In addition to this simple topological consideration, and depending on the contact observation length-scale, there is a wide spectrum of surface and bulk phenomena which add further complications at the contact analysis (see an overview of tribochemistry-field topics in [18]). For the high-pressure mixed-lubrication squeeze problem, the absence of an established research activity should not surprise, as the phenomenon requires to solve the lubrication equation at each time step.

In this section we apply a recent development of the high-pressure transient mixed lubrication theory [12] and [13] in order to analyze the effect of surface roughness on the pin-pulley interaction, which becomes relevant when the minimum lubricant film thickness is of the order of the surface h_{rms} . Indeed in the mixed lubrication regime, the applied load is supported by both fluid-asperity and asperity-asperity interactions, the latter becoming more severe by reducing the average separation between the solids. In the ML model [13] we have basically assumed that the macroscopic contact size (i.e. the Hertzian length for dry interactions) is much

higher than the largest roughness length scale, so that the local, roughness-induced spatial variation of the solution fields has been homogenized through a spatial average, leading to smooth solutions.

Here we show results for a self-affine isotropic roughness described by an $h_{rms} = 0.1 \mu\text{m}$, a fractal dimension $D_f = 2.2$, a roll-off wavevector $q_0 = 0.63 \cdot 10^4 \text{ m}^{-1}$ and a short-distance cut-off wavevector $q_1 = 10^3 q_0$. In Fig. 5 we show the average fluid-substrate interaction, in term of (average) fluid pressure (black solid lines), and the severity of the asperity-asperity interactions, in term of (average) solid pressure (red solid lines), as function of the radial coordinate, for different time steps and for an applied constant load $F_0 = 1 \text{ kN}$.

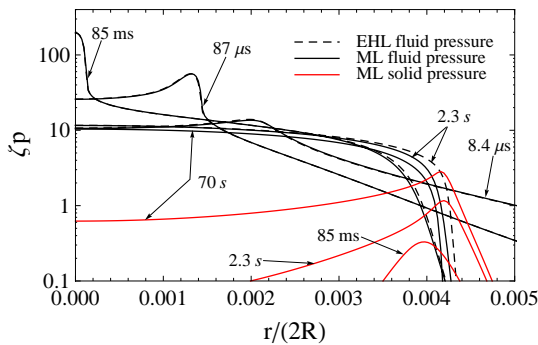


Fig. 5. Fluid and solid pressure fields as functions of radial coordinate, for different squeezing times; the initial central separation is $10 \mu\text{m}$, $h_{rms} = 0.1 \mu\text{m}$ and $F_0 = 1 \text{ kN}$; the EHL fluid pressure for $t = 70 \text{ s}$ is the same as for $t = 2.3 \text{ s}$

The fluid has been modeled with a linear visco-elastic rheological model (of Maxwell type, [8] and [13]), in order to obtain more realistic, smoother fluid pressure peak values (the reader is invited to compare the Newtonian fluid pressure curves of Fig. 2 with the Maxwell fluid pressure curves of Fig. 5). The use of the Maxwell rheology instead of the classical Newtonian rheology introduces only local variations of the fluid pressure field, in correspondence of the annular pressure peak). Note in Fig. 5 that during the pin-pulley traveling time (of order 10^{-2} s) the predictions of the EHL simulation does not differ from ML calculations (ML fluid pressure curves for times less than or equal to 85 ms are superposed to EHL pressure results), as the probability of asperity-asperity interactions, for

separations higher than h_{rms} value, exponentially decreases as separation increases [19]. The contribution from solid contact becomes appreciable only for contact time of order 1 s, where a solid pressure peak is formed and travels towards the contact axis.

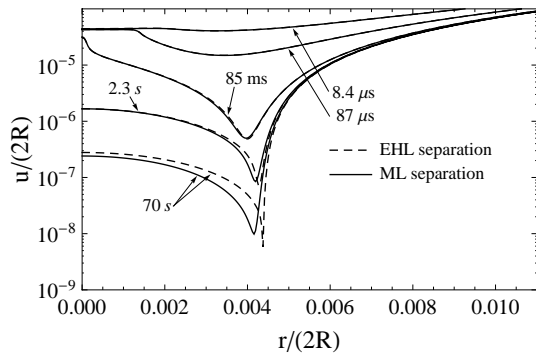


Fig. 6. The interfacial separation as a function of the radial coordinate for different squeeze times.

For EHL and ML analysis; the initial central separation is $10 \mu\text{m}$, $h_{rms} = 0.1 \mu\text{m}$ and $F_0 = 1 \text{ kN}$. The EHL fluid pressure for $t = 70 \text{ s}$ is the same as for $t = 2.3 \text{ s}$.

In Fig. 6 we show the (average) interfacial separation as a function of radial coordinate, and for different time instants, in a linear-log diagram. The correspondence of the radial position of the solid pressure peak with that of the minimum separation is simply justified by considering that the smaller is the separation, the higher is the number of touching asperities so that the higher is the total solid-solid supported load.

Moreover, we also stress how important is the knowledge of the full power-spectral-density (PSD) of the surface roughness (which, in many cases, is an exhaustive information for the complete description of random roughness) for the correct estimation of the time-transition from hydrodynamic to mixed lubrication regime. From dimensionless considerations, the pressure needed to flatten an asperity of height h is of order E^*h/L , where E^* is the asperity elastic modulus and L the asperity wavelength, thus the full PSD, from which the relation h/L can be determined, must be an essential feature of any reasonable (dry or lubricated) contact mechanics theory in order to determine the amount of the solid-solid interaction at a given separation and h_{rms} value [19]. Note also in Fig. 6 that the minimum

separation, for ML, results in an higher value compared to EHL calculation, as it should be expected because of the presence of contacting asperities.

3 THE INFLUENCE OF LOW-SPEED CVT OPERATION ON PIN-PULLEY INTERACTION

In this section we analyze the case of low-speed CVT operations in conjunction with a time-varying, numerically evaluated load history.

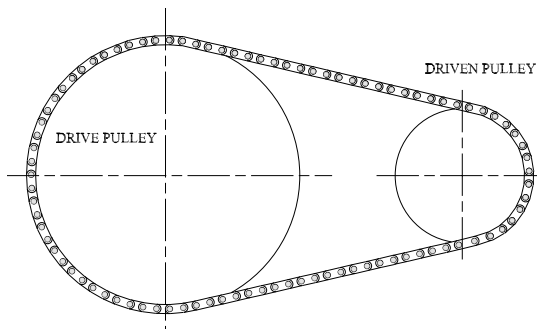


Fig. 7. The multibody model of the chain drive

In Sec. 0 we defined the *PPTT* as the time needed by the pin to travel along the pulley. At a fixed speed ratio, this time is strictly dependent on the drive (or driven) angular velocity and, as it should be expected, there exists a velocity threshold under which the lubrication regime at the pin-pulley contact cannot be fully EHL during all the *PPTT* with obvious consequences on the wear process of the surfaces. Note that the investigation of this problem is of fundamental importance in case of CVTs, as the occurrence of relatively high values of *PPTT* is always encountered during the switch on/off of the transmission.

In order to evaluate the contact loads on each chain pin during the interaction with the pulley sheaves, some of us [20] have realized a discrete multibody model of the chain drive, which we briefly summarize. The model of the metal chain considers a bi-dimensional pin-jointed chain (Fig. 7), where each pin is modeled as a mass point provided with two translational degrees of freedom. Moreover, the chain pins are connected with n links, replaced by massless spring-damper elements. The system of equilibrium equations of the chain pins is numerically integrated forward in time, by

providing the variator with a constant primary speed and a fixed load torque.

The pressure load acting on each pin (non-zero during the pulley contact stages) is expressed as a function of the pin axial stiffness and of its elastic compression, which in turns depends on the pin position and on the elastic deformation of the pulleys. In particular, the pulley deformed groove angle β is modeled by means of the Sattler's sinusoidal approximation [21], while the pin axial stiffness k_p is evaluated as $k_p = E_p A_p / L_p$, where E_p is the steel Young's modulus, which is equal to 206 GPa, $A_p = 12 \text{ mm}^2$ is the pin cross sectional area and $L_p = 30 \text{ mm}$ is the pin length, leading to $k_p = 8.24 \times 10^7 \text{ N/m}$.

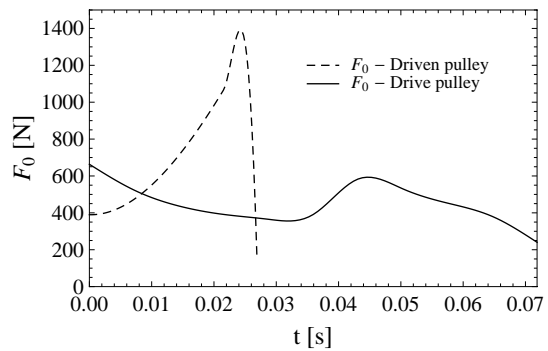


Fig. 8. Normal loads at the pin-pulley interface as functions of time for a CVT running in overdrive at low angular velocities (speed ratio $\tau = 2$)

In Fig. 8 we show the outcomes of the chain model simulations in terms of normal load-time curve which have been evaluated for a CVT variator operating at speed ratio $\tau = 2$, angular velocity of the drive pulley $\omega_{DR} = 50 \text{ rad/s}$ and secondary torque $T_{DN} = 50 \text{ Nm}$. The clamping forces, evaluated with the pin compliant model, oscillate around a mean value respectively equal to $S_{DR} = 12 \text{ kN}$ for the drive pulley and to $S_{DN} = 8 \text{ kN}$ for the driven one. In these loading conditions, the contact force distribution on the drive pulley (see the continuous line in Fig. 8) appears slightly decreasing in the first part of the contact arc while the load sharply increases close to the middle of the wrapping arc. After the peak, the normal force again decreases until the pin leaves the contact with the pulley sheaves. On the driven side, (dashed line in Fig. 8) the normal force shows a monotonic trend from the inlet point to the exit point and it grows up to 1.4 kN.

In this case, indeed, the time of contact is shorter due to the reduced length of the contact arc when the variator transmission ratio is set to overdrive.

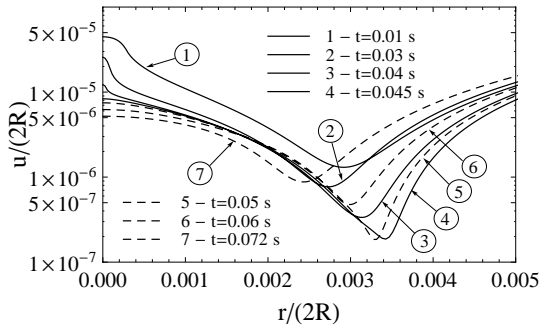


Fig. 9. The film thickness as a function of the radial coordinate for different time instants; drive pulley; the radial displacement of the position of the minimum film thickness during time is due to the corresponding variation of normal load

For the aforementioned load history, we evaluate the pin-pulley squeeze motion experienced on both the drive and the driven pulleys. In Fig. 9 we show the separation field as a function of radial coordinate, for different time instants and for a chain pin in contact with the drive pulley. It is interesting to notice that the minimum film thickness value is not a monotonically decreasing time-function, but reaches a minimum during $t_4 < t < t_5$, exactly when the normal load undergoes the local time-increase, as shown in Fig. 8 by the solid line.

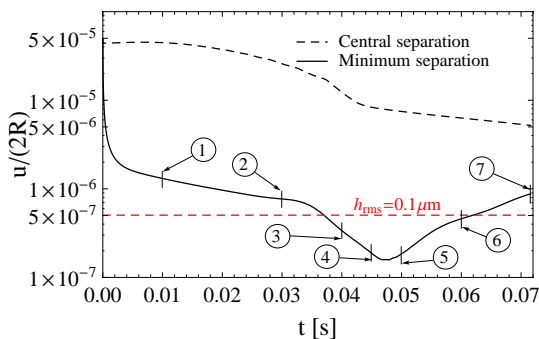


Fig. 10. Central and minimum film thickness as functions of the squeeze time; drive pulley; the enumeration of circles corresponds to the same time instants shown in Fig. 9

In Fig. 10 we show the minimum and central separation as function of time.

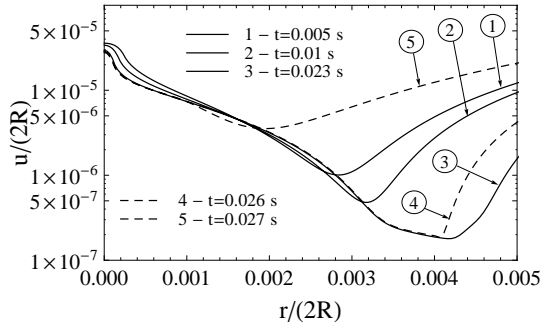


Fig. 11. The film thickness as a function of the radial coordinate for different time instants; driven pulley; the radial displacement of the position of the minimum film thickness during time is due to the corresponding variation of normal load

Note that for a h_{rms} roughness of about 0.1 μm , the pin interaction with the drive pulley is characterized by an initial EHL regime, followed by a ML regime and again an EHL regime. We conclude that very different contact mechanisms describe the pin-pulley interaction at different relative angular positions. From Fig. 9 it is also possible to predict that in such operating conditions the pin should experience wear only in an annular region where the film thickness is smaller than the h_{rms} of the surface.

On the driven pulley the main features of the pin-pulley interaction are similar to those experienced on the drive side, despite the *PPTT* is lower (about 0.027 s). In Fig. 11 we show the film thickness as function of radial coordinate, for different squeeze times (the peak of the normal load occurs between t_3 and t_4). Note that also during the driven-stage three different lubrication regimes are encountered. This is clearly visible in Fig. 12, where we show the central and minimum film thicknesses as functions of time. Note that on the driven pulley, differently from the drive one, the ML regime is experienced in a wider angular domain if compared to the EHL regime.

Therefore we conclude that, in the case of low-speed CVT running conditions, the pin-pulley interaction is not uniquely characterized by an EHL regime. Actually, the lubrication regime may switch from EHL to ML and vice versa depending on the pin-pulley traveling time and on the normal load time-evolution. It results that, despite the macroscopic quantitative prediction of CVT performances is already state-of-art [5] and [6], the quantitative (accurate) modeling of chain-

pulley interaction in such transmissions needs a deeper investigation and modeling of the tribology at pin-pulley interface.

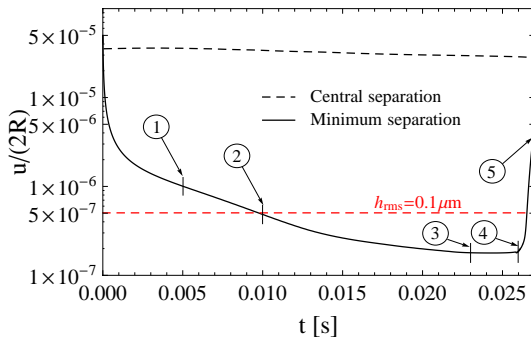


Fig. 12. Central and minimum film thicknesses as functions of squeeze time; driven pulley; the enumeration of circles corresponds to the same time instants shown in Fig. 11

4 CONCLUSION

We investigated the lubrication conditions at the pin-pulley interface in a GCI chain CVT. In particular, we focused on the interaction behavior during normal and low-velocity CVT operations. For a characteristic pin-pulley traveling time of 0.01 s (typical of normal CVT operations), we showed that a h_{rms} surface roughness less than 0.1 μm and a squeezing load of about 1kN, corresponding to the adopted values in such systems, guarantee a fully lubricated EHL regime at the interface. Indeed, a stiff high-viscosity oil dimple is generated in the middle of the junction which is able to avoid the surfaces from being in direct asperity-asperity contact during all the PPTT.

In the case of low-velocity CVT operations, we showed that due to a larger PPTT (respect to the typical 10^{-2} s value) the pin-pulley interaction is no more uniquely characterized by a single EHL regime (or an EHL regime to be followed by a ML regime), but alternating elasto-hydrodynamic and mixed lubrication stages are experienced by the pin depending on the pin-pulley traveling time and on the normal load time-evolution. We conclude that a deep theoretical/experimental investigation of the contact tribology is still required to quantitatively describe the chain-pulley interaction in CVT transmissions.

5 ACKNOWLEDGEMENTS

The authors would also like to thank Gear Chain Industrial B.V. - Neunen (NL).

6 NOTATION

h_{rms}	Root-mean-square roughness [m]
k_p	Pin axial stiffness [N/m]
p	Pressure [Pa]
q_0	Long-wave cut-off frequency [m^{-1}]
q_1	Short-wave cut-off frequency [m^{-1}]
t	Time [s]
u	Interfacial separation [m]
A_p	Pin cross sectional area [m^2]
D_f	Fractal dimension
E_p	Steel Young modulus [Pa]
F_0	Normal load [N]
L_p	Pin length [m]
$PPTT$	Pin-pulley traveling time [s]
R	Equivalent contact radius [m]
S_{DN}	Driven pulley clamping force [N]
S_{DR}	Drive pulley clamping force [N]
T_{DN}	Secondary torque [Nm]
β	Pulleys groove angle
ζ	Piezoviscosity coefficient [Pa^{-1}]
τ	CVT speed ratio
ω_{DR}	Drive pulley angular velocity [rad/s]

7 REFERENCES

- [1] Carbone, G., Mangialardi, L., Mantriota, G. (2001) Fuel consumption of a mid class vehicle with infinitely variable transmission lubrication, *SAE Transactions - Journal of Engines*, vol. 110, no. 3, p. 2474-2483.
- [2] Carbone, G., Mangialardi, L., Mantriota, G., Soria, L. (2004) Performance of a city bus equipped with a toroidal traction drive, *IASME Transactions*, vol. 1, no. 1, p. 16-23.
- [3] Mantriota, G. (2005) Fuel consumption of a vehicle with power split CVT system, *Int. J. Veh. Des.*, vol. 37, no. 4, p. 327-342.
- [4] Simons, S.W.H., Klaassen, T.W.G.L., Steinbuch, M., Veenhuizen, P.A., Carbone, G. (2008) Shift dynamics modelling for optimization variator slip control in a push-belt CVT, *Int. J. Veh. Des.*, vol. 48, no. 1-2, p. 45-64.
- [5] Carbone, G., Mangialardi, L., Mantriota, G. (2005) The influence of pulley deformations

- on the shifting mechanisms of MVB-CVT, *ASME J. Mech. Des.*, vol. 127, p. 103-113.
- [6] Carbone, G., Mangialardi, L., Bonsen, B., Tursi, C., Veenhuizen, P.A. (2007) CVT dynamics : Theory and experiments, *Mechanism and Machine Theory* 42(4), p. 409-428.
- [7] Carbone, G., Scaraggi, M., Soria, L. (2009) The lubrication regime at pin-pulley interface in chain CVTs, *ASME J. Mech. Des.*, vol. 131, no. 1, 011003.
- [8] Carbone, G., Scaraggi, M., Mangialardi, L. (2009) EHL-squeeze at pin-pulley interface in CVTs: Influence of lubricant rheology, *Tribology International*, vol. 42, no. 6, p. 862-868.
- [9] Sniik, J., Pfeiffer, F. (1997) Dynamics of CVT chain drives: mechanical model and verification, *ASME*, Paper No. DETC97/VIB-4127.
- [10] Saito, T. (2007) Simulation of stress on elements of CVT metal pushing V-belt under transient operating conditions, *Proceedings of the International Congress on Continuously Variable and Hybrid Transmissions*, Yokohama, Paper no. 20074544.
- [11] Kanehara, S., Fujii, T., Kitagawa, T. (1994) A study of a metal pushing V-belt type CVT-Part 3: What forces act on metal blocks?, *SAE Paper no. 940735*.
- [12] Persson, B.N.J., Scaraggi, M. (2009) On the transition from boundary lubrication to hydrodynamic lubrication in soft contacts, *J. Phys.: Condens. Matter*, vol. 21, 185002 (22pp).
- [13] Scaraggi, M., Carbone, G. (2009) Transition from elastohydrodynamic to mixed lubrication in high loaded squeeze contacts, *Journal of the Mechanics and Physics of Solids*, submitted (2009).
- [14] Dowson, D. (1998) Modelling of Elastohydrodynamic Lubrication of Real Solids by Real Lubricants, *Meccanica*, vol. 33, p. 47-58.
- [15] Sivebaek, I.M., Samoilov, V.N., Persson, B.N.J. (2004) Squeezing molecularly thin alkane lubrication films: layering transitions and wear, *Tribology Letters*, vol. 16, no. 3, p. 195-200.
- [16] Zhang, C. (2005) Research on thin film lubrication: state of the art, *Tribology International*, vol. 38, p. 443-448.
- [17] Venner, C.H., Lubrecht, A.A. (2000) Multigrid techniques: a fast and efficient method for the numerical simulation of elastohydrodynamically lubricated point contact problems, *Proc Instn. Mech. Engrs. Part J* 214, p. 43-62.
- [18] Hsu, S.M. (2004) Molecular basis of lubrication, *Tribology International*, vol. 37, p. 553-559
- [19] Persson, B.N.J. (2007) Relation between Interfacial Separation and Load: A General Theory of Contact Mechanics. *PRL* 99, 125502.
- [20] De Novellis, L., Carbone G., (2009) Numerical comparison between a continuous and multibody model in CVT chain transmissions. *To be submitted*.
- [21] Sattler, H. (1999) Efficiency of Metal Chain and V-Belt CVT. *Proceedings of the International Congress on Continuously Variable Transmission*, Eindhoven, p. 99-104.